Inorganic Chemistry

Article

pubs.acs.org/IC

Transferrin Serves As a Mediator to Deliver Organometallic Ruthenium(II) Anticancer Complexes into Cells

Wei Guo, Wei Zheng, Qun Luo, Xianchan Li, Yao Zhao, Shaoxiang Xiong, and Fuyi Wang*

Beijing National Laboratory for Molecular Sciences, CAS Key Laboratory of Analytical Chemistry for Living Biosystems, Beijing Centre for Mass Spectrometry, Institute of Chemistry, Chinese Academy of Sciences, Beijing 100190, PR China

Supporting Information

ABSTRACT: We report herein a systematic study on interactions of organometallic ruthenium(II) anticancer complex $[(\eta^6\text{-arene})Ru(en)Cl]^+$ (arene = *p*-cymene (**1**) or biphenyl (**2**), en = ethylenediamine) with human transferrin (hTf) and the effects of the hTf-ligation on the bioavailability of these complexes with cisplatin as a reference. Incubated with a 5-fold excess of complex **1**, **2**, or cisplatin, 1 mol of diferric hTf (holo-hTf) attached 0.62 mol of **1**, 1.01 mol of **2**, or 2.14 mol of cisplatin. Mass spectrometry revealed that both ruthenium complexes coordinated to N-donors His242, His273, His578, and His606, whereas cisplatin bound to O donors Tyr136 and Tyr317 and S-donor Met256 in addition to His273 and His578 on the surface of both apo- and holo-hTf. Moreover, cisplatin could bind to Thr457 within the C-lobe iron binding cleft of apo-hTf. Neither ruthenium nor platinum binding interfered with the recognition of holo-hTf by the transferrin receptor (TfR). The ruthenated/platinated holo-hTf complexes could be internalized via TfR-mediated endocytosis at a similar rate to that of holo-hTf itself. Moreover, the binding to holo-hTf well preserved the bioavailability of the ruthenium complexes, and the hTf-bound **1** and **2** showed a similar cytotoxicity toward the human breast cancer cell line MCF-7 to those of the complexes themselves. However, the conjugation with holo-hTf significantly reduced the cellular uptake of cisplatin and the amount of platinated DNA adducts formed intracellularly, leading to dramatic reduction of cisplatin cytotoxicity toward MCF-7. These findings suggest that hTf can serve as a mediator for the targeting delivery of Ru(arene) anticancer complexes while deactivating cisplatin.

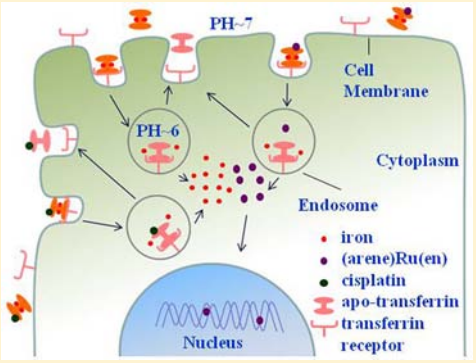

INTRODUCTION

The transferrins are a family of single-chain glycoproteins, being typified by serum transferrin, the iron transport protein in blood. Human transferrin (hTf) contains 679 amino acid residues with a molecular weight of ~79 kD, and the molecule is stabilized by 19 intrachain disulfide bonds and is protected by three carbohydrate side chains.[1−3] The polypeptide chain of hTf is folded into two structurally similar but functionally different lobes, designated the N-lobe and C-lobe, which are linked by a short spacer sequence. Each lobe can be further divided into two domains enclosing a deep hydrophilic cleft housing an iron binding site which consists of four conserved amino acids including two tyrosines, one aspartic acid, and one histidine. The conformational change induced by iron(III) binding is more pronounced in the N-terminal lobe than the C-terminal lobe due to the presence of an additional disulfide bond, which restricts the cleft opening as much as that of the N-terminal lobe in the absence of iron(III).[4−7] The C-terminal lobe binds to Fe^{3+} more strongly than the N-terminal site, and it is also the last lobe to release Fe^{3+} via a process induced by reduced pH.[2] Certain aberrant cells, in particular, cancer cells, require a high level of iron(III) in order to facilitate rapid cell growth, which is satisfied by upregulating the expression of TfR on the cell surface and thereby sequestering a greater amount of the circulating metal-loaded hTf. Accordingly, there is a potential use of hTf as a ligand for metal-based chemotherapeutic and diagnostic agents such as ruthenium(III),[8−10] gallium(III),[11−14] indium,[4,15] and titanium(IV)[16,17] complexes because the heterometal−transferrin complexes are still recognized by TfR, allowing the targeted delivery of the metallodrugs to cancer cells via TfR-mediated endocytosis.[18−20]

The success of cisplatin and other platinum anticancer drugs has stimulated a renaissance of inorganic medicinal chemistry and the search for complexes of other transition metals with interesting biological properties.[21−23] Among the large number of nonplatinum transition metal compounds tested for chemotherapeutics, Ru-based compounds have attracted increasing attention because the well-known octahedral Ru center provides many synthetic opportunities for tuning the biological activities of inorganic pharmaceuticals by organizing a wide range of ligands in the three-dimensional space.[10,21,24,25] Two ruthenium(III) complexes, [ImH][*trans*-$RuCl_4$(DMSO)-(Im)] (NAMI-A, Im = imidazole)[26] and indazolium *trans*-[tetrachlorobis(1*H*-indazole)Ru] (KP1019),[27] which exhibit good inhibitory efficacy on pulmonary metastases in all the solid tumors and antitumor activity versus several human colon carcinoma cell lines,[28] respectively, have recently completed

Received: February 1, 2013
Published: April 15, 2013

   dx.doi.org/10.1021/ic4002626 | *Inorg. Chem.* 2013, 52, 5328−5338

phase I clinical trials.[10] More recently, two groups of organometallic ruthenium(II) complexes, $[(\eta^6\text{-arene})Ru(en)(Cl)]^+$ (arene = *p*-cymene, biphenyl, tetrahydroanthrance, etc., en = ethylenediamine)[29−31] and $[(\eta^6\text{-arene})RuCl_2(pta)]$ (pta =1,3,5-triaza-7-phosphatricyclo[3.3.1.1]decane,[32,33] have shown interesting anticancer activities. The former group exhibits cytotoxicity both in vitro and in vivo and is even cytotoxic toward cisplatin-resistant cancer cell lines.[29−31] The majority of the latter group is only weakly active or inactive in vitro but shows highly selective activity against metastases in vivo.[10,22]

Both in vivo and in vitro research have demonstrated that following intravenous administration, Pt- and Ru-based anticancer complexes can bind extensively to serum proteins, in particular albumin and transferrin, playing a crucial role in the drug transport and metabolism.[2,34] There have been numerous reports on the investigation of interactions between cisplatin,[35−37] ruthenium(III) anticancer complexes,[8,9,38] and serum proteins. And hTf has been shown to be involved in the transport, metabolism, and action of Ru^{III} anticancer complex KP1019.[8,10,39] However, few reports on the interactions between ruthenium(II) arene anticancer/antimetastasis complexes and transferrin have been published.[40] Also, the coordination chemistry and biological roles of the interactions between organometallic ruthenium anticancer complexes and transferrin remain poorly understood.

In the present work, with cisplatin as a reference, the interactions between ruthenium(II) arene anticancer complex $[(\eta^6\text{-arene})Ru(en)Cl]^+$ (arene = *p*-cymene (*p*-cym, **1**) or biphenyl (bip, **2**), en = ethylenediamine) and human transferrin in both apo and holo forms have been studied by the combination of electrospray ionization mass spectrometry coupled to high performance liquid chromatography (HPLC-ESI-MS), tryptic digestion of the metalated protein complexes, and molecular modeling. The effects of these interactions on the hTf-TfR recognition and on the bioavailability and cytotoxicity of the tested anticancer complexes were subsequently explored using receptor assay, inductively coupling plasma mass spectrometry (ICP-MS), and in vitro cytotoxicity assay, respectively.

EXPERIMENTAL SECTION

Materials. The complexes $[(\eta^6\text{-arene})Ru(en)Cl][PF_6]$ (arene = *p*-cymene (**1**$[PF_6]$) or biphenyl (**2**$[PF_6]$), en = ethylenediamine, Chart 1) were synthesized as described in the literature.[30] Cisplatin was purchased from Alfa Aesar. Apo and holo transferrin were purchased from Calbiochem (U. S. A.) and extensively dialyzed against NH_3HCO_3 buffer (100 mM) and lyophilized prior to use. Human tetramethylrhodamine-labeled human transferrin (TMR-hTf) was purchased from Invitrogen, trypsin (sequence grade) from Promega, guanidine hydrochloride from Amresco, iodoacetamide and acetonitrile (HPLC grade) from Merck, formic acid (FA) from Acros, selenocystamine dihydrochloride from Sigma, dithiothreitol (DTT) from Pierce, triethylammonium acetate buffer (TEAA) from Transgenomic, 3-(4,5-dimethyl-2-thiazolyl)-2,5-diphenyl-2H-tetrazolium bromide (MTT) from Sigma, and HNO_3 (BV−III grade) from BICR (Beijing, China). Microcon centrifugal filtration units with a 10 kDa molecular weight cutoff were purchased from Millipore. Tissue culture reagents were obtained from HyClone. Aqueous solutions were prepared using Milli-Q water (Milli-Q Reagent Water System).

Chart 1. Chemical Structures of the Organometallic Ruthenium Complexes Studied in This Work

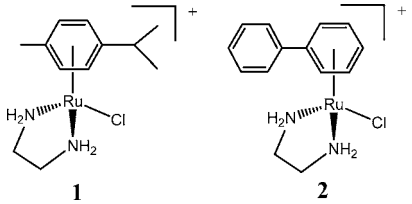

1 **2**

Preparation of Metalated hTf Adducts. In a typical reaction, apo- or holo-hTf (100 μM) in 20 mM TEAA (pH 7.4) was incubated with ruthenium complexes **1**, **2**, or cisplatin at a molar ratio of 1:5 for 48 h at 310 K. Unbound ruthenium complexes **1** and **2** and cisplatin were removed by three rounds of centrifugal filtration with a 10 kDa cutoff filter at 5000*g* for 12 min at ambient temperature, giving rise to respective metalated hTf adducts. The metalated TMR-holo-hTf adducts were prepared by a similar procedure to that described above.

Trypsin Digestion and in Silico Digestion of hTf and Metalated hTf Adducts. The hTf, ruthenated, or platinated hTf adducts (50 μL, 20 μM) were mixed with 450 μL of denaturing buffer (pH 8.5) containing guanidine hydrochloride (6 M), NH_4HCO_3 (100 mM), 2.5 μL DTT (1.0 M in 100 mM NH_4HCO_3 buffer, pH 8.2), and 3 μL selenocystamine dihydrochloride (100 mM in water). The resulting solution was incubated at 310 K for 30 min to cleave the disulfide bonds. Then, iodoacetamide (6 μL, 1.0 M in 1.0 M NaOH) was added, and the resulting mixture was incubated in the dark for another 30 min at ambient temperature to alkylate the free thiol groups. The resulting solution was then dialyzed against NH_4HCO_3 buffer (100 mM, 1 L, pH 7.8) for 2 h at ambient temperature. An aliquot of the dialyzed sample was mixed with 2 μg of trypsin, giving a substrate/enzyme ratio of 40:1, and then was incubated at 310 K for 18 h for digestion. The tryptic digests of hTf or metalated hTf adducts were separated on the C18 column, and the fractions were subsequently analyzed by mass spectrometry. In silico tryptic digestion of hTf was used to identify peptides. The theoretical *m*/*z* values of tryptic digestion of hTf were generated by the "MS-Digest" program (http://prospector.ucsf.edu). Cysteines were set as carboxyamidomethyl-cysteines; peptide masses were calculated as monoisotope and multiple charges.

Electrospray Ionization Mass Spectrometry Coupled with High Performance Liquid Chromatography (HPLC-ESI-MS). Positive-ion electrospray ionization mass spectra were obtained on a Micromass Q-TOF mass spectrometer (Waters) coupled to a Waters CapLC system. The tryptic digests of hTf or metalated hTf adducts were separated on a Symmetry-C18 column (1.0 × 50 mm, 100 Å, 3.5 μm, Waters). Mobile phases were (A) 95% H_2O containing 4.9% acetonitrile and 0.1% formic acid and (B) 95% acetonitrile containing 4.9% H_2O and 0.1% formic acid. The peptides were eluted with a 50 min linear gradient from 1% to 45% of B at a rate of 30 μL min^{-1}. The eluent was directly infused into the mass spectrometer through the ESI probe. The spray voltage of the mass spectrometer was 3.30 kV and the cone voltage 35 V. The desolvation temperature was 413 K and source temperature 353 K. Nitrogen was used as both cone gas and desolvation gas with a flow rate of 40 L h^{-1} and 400 L h^{-1}, respectively. The collision energy was set to 10 V. The MS spectra were acquired in the range of 500−1800 *m*/*z*. The mass accuracy of all measurements was within 0.001 *m*/*z* unit, and all *m*/*z* values corresponding to the mass-to-charge ratios of the most abundant isotopomer of the observed ions were calibrated first versus a NaI calibration file and then the respective native peptides. Mass Lynx (ver. 4.0) software was used for analysis and post processing.

Receptor Assay. The binding of ruthenated or platinated hTf to the transferrin receptor was characterized by Enzyme-Linked Immunosorbent Assay (ELISA). Each well of a microlitre plate was coated by incubation with 100 μL of 10 μg mL^{-1} transferrin receptor (11020-H07H, Sino Biological) in phosphate buffered saline (PBS) overnight at 277 K. Thorough washing was made with PBS. Then, all wells of the plate were blocked with 200 μL of 2% bovine serum albumin (BSA) in PBS at 310 K for 2 h, followed by three rounds of washing with PBS prior to use. Next, 100 μL of hTf or metalated hTf adducts at various concentrations, ranging over 0, 0.0032, 0.0016, 0.08, 0.4, 2, and 10 μg(hTf) mL^{-1}, in 0.2% BSA were loaded, and the plate

dx.doi.org/10.1021/ic4002626 | Inorg. Chem. 2013, 52, 5328−5338

was incubated at 310 K for 1 h. Following three rounds of washing with PBS, 100 μL/well of mouse antihuman Tf-mAb (1 μg mL^{-1}) in 0.2% BSA was added, and the plate was incubated for half an hour at 310 K and then washed with PBS three times. Revelation was made with 100 μL of antimouse lgG(F(ab)2)/HRP (1 μg mL^{-1}) in 0.2% BSA solution at 310 K for half an hour. All wells were thoroughly washed, followed by the addition of 200 μL/well of TMB substrate solution and incubated at 310 K for a further 20 min. The reaction was stopped by the addition of 100 μL of 2 M H_2SO_4, and the plate was then read on a SpectraMax M5 Reader (Molecular Devices, USA) at 450 nm. All experiments were performed in triplicate.

Cell Culture. Human breast adenocarcinoma cell line, MCF-7, was originally received from the American Type Culture Collection (ATCC) and cultured in monolayers in Advanced DMEM (High Glucose), supplemented with antibiotic (100 U mL^{-1} penicillin and 100 U mL^{-1} streptomycin) and 10% fetal bovine serum (HyClone, South American Origin). This fully supplemented medium is referred to below as growth medium. The cells were seeded at a density of 5×10^6 cells per 100 mm Petri dish (8 mL of growth medium), grown to 80−90% confluency at 310 K in a 5% CO_2-humidified incubator, and subcultured every 2 days, using standard cell culture procedures.

Fluorescent Confocal Imaging. First, 1×10^5 cells in 1.5 mL of growth medium were deposited into a Petri glass-bottom dish and allowed to attach for 12 h. By replacing the medium with fresh medium, cells were treated with TMR-holo-hTf or metalated TMR-holo-hTf adducts at a concentration of 5×10^{-7} M (hTf) at 310 K for 2 h. The culture medium was removed and the cells washed with PBS three times, and 1.5 mL of PBS solution was then added to each dish. The confocal fluorescence images of TMR were captured using an IX81 inverted microscope (Olympus, Tokyo, Japan) equipped with an FV1000 scanning unit and a 559-nm FV10-LD559 laser.

Cellular Uptake. Cells were plated at a density of 5×10^6 cells/100 mm Petri dish in 8 mL of culture medium on day 1. On day 2, cells were exposed to the Ru/Pt compounds or the metalated hTf adducts at a concentration of 20 μM (Ru or Pt). Stock solutions (1 mM) of the metal complexes or the metalated hTf adducts were made up freshly in PBS before being diluted in media to give a final concentration of 20 μM. After 1, 6, or 24 h of treatments with tested compounds or protein adducts, cells were trypsinized and the cell suspension counted using a cell counting chamber (Qiujing, Beijing). One third of the cells were centrifuged, washed with PBS, and stored at 277 K for the determination of metal concentration in whole cells by ICP-MS. One third of the cells were used for DNA extraction using the Nucleon genomic DNA extraction kit (Tiangen Biotech, Beijing). The DNA extraction was resuspended in a final volume of 1 mL of water, and the concentration of DNA was measured at 260 nm using a UV−vis spectrophotometer (Shimadzu, Japan) before the determination of metal content by ICP-MS. The last one-third of cells were used for protein extraction using the RIPA Lysis Buffer (Bioteke Corporation, Beijing). The extracted proteins were resuspended in a final volume of 1 mL of water, and the total concentration of proteins was measured with a BCA protein assay kit (Tiangen Biotech, Beijing) prior to the measurement of the metal content by ICP-MS.

Inductively Coupled Plasma Mass Spectrometry (ICP-MS). To the whole cell pellets, protein, or DNA extracts, 0.5 mL 50% (v/v) HNO_3 was added; the solutions were sonicated for 10 min and then transferred to 20 mL conical flasks. The containers were washed three times with a total of *ca.* 4 mL of 20% nitric acid, and the wash was also added to the 20 mL flasks. The flasks were heated on a hot plate for 30−40 min until the solutions became clear, were allowed to cool, and then were further heated at the boiling point for 30−40 min with the addition of 4 mL of deionized water. For each sample, the resulting digested solution was transferred to a volumetric tube, and the conical flask was washed with deionized water three times. The washes were added to the initial digests. The solution volume was increased to 5 mL with deionized water and stored at 277 K for ICP-MS analysis. Ruthenium and platinum determination by ICP-MS was carried out on an Elan DRC-e ICP-MS (PerkinElmer, U. S. A.). The Ru and Pt standards (NCS Analytica Instruments, 1000 μg mL^{-1} in 10% HCl) were diluted with deionized water to 10 μg mL^{-1} as the stock solution, and the standards for calibration were freshly prepared by diluting this stock solution with 1% HNO_3. The concentrations used for calibration were 0.1, 1, 10, and 100 pg (Ru and Pt) mL^{-1}. During sample analysis, resloping was performed once for every 10 samples using the 1 pg mL^{-1} standard. All experiments were performed in triplicate.

In Vitro Cytotoxicity Assay. The in vitro cytotoxicity of complexes **1**, **2**, and cisplatin as well as the metalated hTf adducts toward the MCF-7 cell line was measured by MTT assay. A suspension of cells (4000/well in 100 μL) was plated in 96-well plates and cultured for 12 h, and then the free complexes or metalated hTf adducts, which range evenly from 100, 25, 6.25, 1.5625, 0.39063, 0.09766, 0.02441, and 0 μM, were added to the corresponding plates. The plates were subsequently incubated at 310 K for 72 h in a CO_2 incubator. After the treatments, the culture medium was removed, and the plates were washed with PBS three times, followed by the addition of fresh medium. Then, 25 μL of MTT solution (5 mg mL^{-1} in PBS) was added to each well. MTT is reduced to purple formazan in living cells by mitochondrial reductase. After 4 h of incubation at 310 K, the MTT/medium was removed carefully, and DMSO (100 μL) was added to each well to dissolve the formazan crystals. The absorbance of each well was determined by a SpectraMax M5 Reader at 490 nm. Cell viability was expressed as a percentage of the control. All experiments were performed in triplicate.

Molecular Modeling. The molecular models were constructed using the Sybyl X 1.1 program (Tripos Inc.) running on a 2.60 GHz dual-core Intel(R) E5300 CPU with 2 GB of RAM under the Windows XP system. The initial crystal structures of apo- and holo-hTf (PDB codes: 3QYT and 2HAV) were obtained from Protein Data Bank and those of complexes **1** and **2** (codes: CCDC170360, CCDC170362) from the Cambridge Crystallography Data Centre. The molecular structure of cisplatin was constructed using the Sybyl program. All of the aqua molecules in the crystal structure of hTf were removed first, and then the ruthenium complexes and cisplatin units were individually docked onto the binding sites of the targeted proteins as identified by mass spectrometry with ruthenium coordinating to the S atom of cysteine or methionine, or to the O atom of the tyrosine residue. The initial coordinative bond distances of Ru−N and Ru−O were set to 2.40 and 2.20 Å, respectively. All the hydrogen atoms were added to define the correct configuration and tautomeric states, and Kollman All charges were added to the biopolymer and Gasteiger−Marsili charges to the ruthenium complexes and cisplatin fragments. All of the atoms were set as the Kollman All type. With standard set parameters, the models were energy-minimized stage by stage using the Kollman All-Atom force field with the Powell energy minimization algorithm, distance dependent dielectric function, and current charges with the constringent energy gradient of 0.05 kcal mol^{-1}, generating the respective molecular model.

RESULTS

Identification of Tryptic Peptides of hTf. First, the native human serum transferrin (hTf) was digested by trypsin, and the tryptic digestion was then analyzed by HPLC-ESI-MS analysis. By matching the mass of the observed tryptic peptides to that of the tryptic peptides of hTf generated by in silico digestion, 50 peptides were identified, designated T1−T50 (Table S1 in the Supporting Information). These peptides cover approximately 75% of the protein sequence. Notably, the peptide T45 at m/z 1180.818 (z = 4+) is a glycopeptide and contains residues Gln603 through Arg623 and the oligosaccharide Hex5HexNAc4NeuAc2 linked to Asn611, in line with the previous report.[41]

Binding Stoichiometry of Ruthenium Arene Complexes and Cisplatin to hTf. Ruthenium complexes **1** and **2** (Chart 1) and cisplatin individually reacted with holo-hTf at a 5:1 molar ratio of Ru/Fe_2hTf or Pt/Fe_2hTf in TEAA buffer to prepare the ruthenated or platinated hTf adducts. After removal

dx.doi.org/10.1021/ic4002626 | *Inorg. Chem.* 2013, 52, 5328−5338

of the unbound ruthenium complexes or cisplatin from the reaction mixtures, the ICP-AES analysis of the resulting metalated proteins indicated that 1 mol of hTf attached 0.62 mol of complex **1**, 1.01 mol of complex **2**, and 2.14 mol of cisplatin, respectively. The results also demonstrate that the ruthenation and platination have little influence on the iron(III) binding to hTf; each hTf molecule still binds to two Fe^{3+}'s (Table 1).

Table 1. Metal Fractions (mol/mol (hTf)) in Native Transferrin and Metalated Transferrin Adducts, Designated as hTf+1, hTf+2, and hTf+3 (3 = Cisplatin), Produced by the Reaction of Transferrin with 5-Fold Excess of Ruthenium Arene Complex 1, 2, or Cisplatin (3) at 310 K for 48 h

	Fe	Ru	Pt
hTf	2.00	0	0
hTf+**1**	1.98	0.62	0
hTf+**2**	2.00	1.01	0
hTf+**3**	1.98	0	2.14

Binding Sites of Ruthenium Arene Complexes and Cisplatin to hTf. The tryptic digestion of the ruthenated or platinated holo-hTf adducts described above was analyzed by electrospray-ionization mass spectrometry coupled to high performance liquid chromatography (HPLC-ESI-MS). Comparing the peptide mass fingerprints (PMFs) of the ruthenated hTf adducts with those of the native protein (Table S1), four ruthenated peptides arising from tryptic digestion of the ruthenated hTf by complex **1** or **2** were identified (Table S2). The isotopic simulations (Figure 1a–d) indicated that the doubly charged ions at m/z 992.462 and 940.924, the triply charged ion at m/z 788.700, and the quadruply charged ion at m/z 1254.747 are assignable to ruthenated peptides T15, T42, T18, and T45, attaching a ruthenium moiety $\{(\eta^6\text{-}p\text{-cym})\text{Ru(en)}\}^{2+}$ (**1′**), respectively. On the basis of the signal intensity of the ruthenated peptide ions (Figure 1a–d), the major binding site for **1** is located in T18, which contain residuess Asp260 through Lys276. It is notable that the peptide T45, which houses the glycosylated site Asn611, was the second abundant ruthenated peptide by **1** and that ruthenation to this peptide had no effect on the glycosylation at Asn611. A similar binding profile to holo-hTf was observed by analysis of the tryptic digest of the ruthenated holo-hTf by **2** (Figure 1e–h, Table S2).

The binding pattern of cisplatin to holo-hTf is very different from that of the ruthenium arene complexes. Five platinated peptides (Figure 2a–e, Table S3) were detected by analyzing the tryptic digest of the platinated holo-hTf complex by cisplatin. According to the signal intensity of platinated peptide ions (Figure 2), the peptide T18, which was identified as the most abundant ruthenated peptide (*vide supra*), is also the most abundant platinated peptide. It is worth mentioning that the total signal intensity of the five platinated peptides by cisplatin is significantly higher than that of the four ruthenated peptides by ruthenium complex **1** or **2** (Figures 1 and 2), indicating that cisplatin binds more strongly to holo-hTf than complex **1** or **2**, in good agreement with the ICP-AES data (*vide supra*).

The metalated apo-hTf adducts were also prepared by reactions of apo-hTf with the tested metal complexes under the same conditions described earlier, and the protein complexes were then analyzed by HPLC-ESI-MS following tryptic

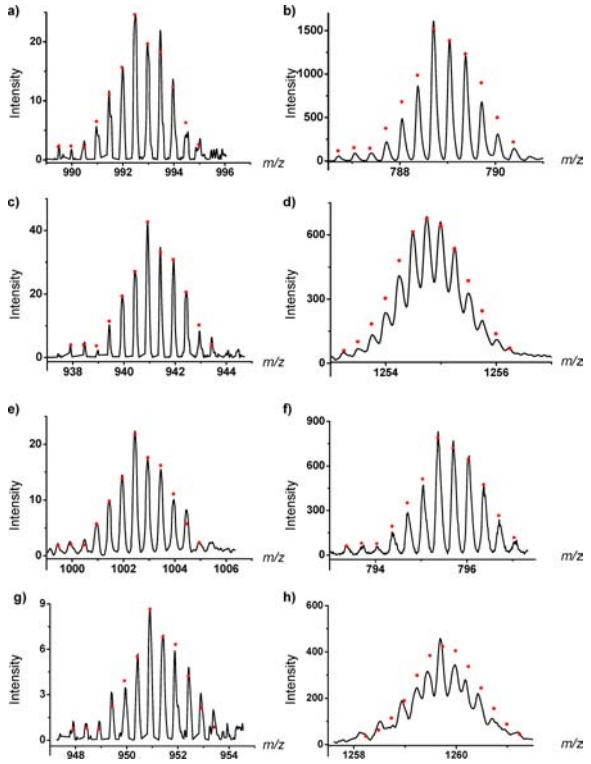

Figure 1. Mass spectra (lines) and isotopic models (dots, for which the values of x and y correspond to the m/z value and intensity of the isotopic ion peaks, respectively) for ruthenated peptides arising from tryptic digestion of ruthenated holo-hTf adducts by complex **1** or **2**: (a) T15+**1′**, (b) T18+**1′**, (c) T42+**1′**, (d) T45+**1′**, (e) T15+**2′**, (f) T18+**2′**, (g) T42+**2′** and (h) T45+**2′**. T15 = (aa240)-DC°HLAQVPSHTVVAR(aa254), T18 = (aa260)-EDLIWELLNQAQEHFGK(aa276), T42 = (aa569)-KPVEEYANC°HLAR(aa581), T45 = (aa603)-Q*QQHLFGSN**VTDC°SGNFC°LFR(aa623). (○) indicates that the cysteine residue was carboxyamidomethylated. (∗) indicates this residue (Gln) was converted to pyro-Glu. (∗∗) indicates the glycosylated site to which a carbohydrate unit (Hex5HexNAc4-NeuAc2) attaches. **1′** = $\{(\eta^6\text{-}p\text{-cym})\text{Ru(en)}\}^{2+}$, **2′** = $\{(\eta^6\text{-bip})\text{Ru-(en)}\}^{2+}$.

digestion. The MS results showed that the binding profiles of complexes **1** and **2** to apo-hTf are identical to those of the complexes to holo-hTf (data not shown). However, apart from the five platinated peptides identified from the platinated holo-hTf, an additional platinated peptide T34, which contains residues Thr457 through Lys470, was observed in the tryptic digest of the platinated apo-hTf complex (Figure 2f).

The ruthenium arene complex $[(\eta^6\text{-bip})\text{Ru(en)Cl}]^+$ (**2**) has shown an adequate affinity to soft Lewis bases cysteine,[42,43] methionine,[42] and borderline base histidine,[44,45] and the coordination with the hard Lewis base carboxyl group of the glutamic acid residue in glutathione (GSH) is not thermodynamically favored.[43] Taking into account that the ruthenated hTf adducts were prepared by 48 h of reaction and all cysteinyl residues in hTf form disulfide bonds, the potential ruthenation sites in hTf are most probably histidine and methionine residues exposed in the protein surface. There are two histidines (His242 and His249) in the ruthenated peptide T15, while there is only one histidine residue in each of the rest of ruthenated peptides T18, T42, and T45. On the basis of the X-ray crystal structure of apo- and holo-hTf,[7,46] we calculated the solvent accessible area (SAA) of the N atoms of the

dx.doi.org/10.1021/ic4002626 | Inorg. Chem. 2013, 52, 5328–5338

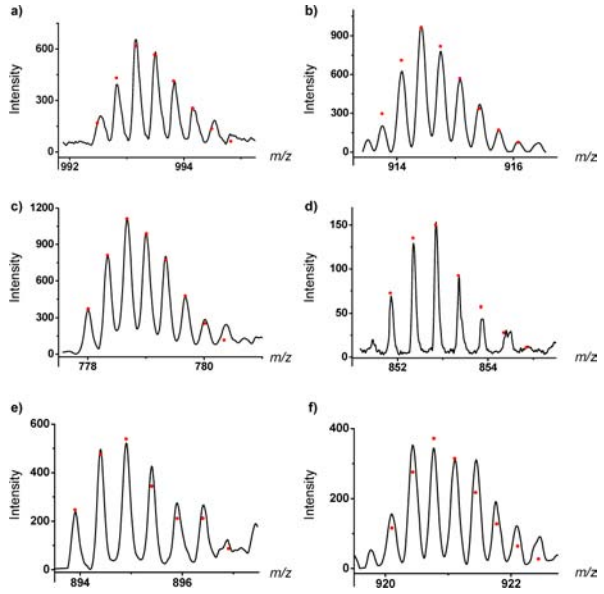

Figure 2. Mass spectra (lines) and isotopic models (dots, for which the values of x and y correspond to the m/z value and intensity of the isotopic ion peak, respectively) for platinated peptides (a) T10+**4**, (b) T16+**4**, (c) T18+**3**′, (d) T24+**4**′, and (e) T43+**3**′ arising from tryptic digestion of platinated holo-hTf by cisplatin (**3**), and (f) T34+**4** arising from tryptic digestion of platinated apo-hTf. T10 = (aa125)-SAGWNIPIGLLYC°DLPEPRKPLEK(aa148), T16 = (aa255)-SMGGKEDLIWELLNQAQEHFGK(aa276), T18 = (aa260)-EDLIWELLNQAQEHFGK(aa276), T24 = (aa313)-MYLGYEYVTAIRNLR(aa327), T43 = (aa569)KPVEEYANC°HLARAPNHAVVTR(aa590), T34 = (aa457)-TAGWNIPMGLLYNK(aa470). (○) indicates that the cysteine residue was carboxyamidomethylated. **3**′ = $\{(NH_3)_2PtCl\}^+$, **3**″ = $\{(NH_3)_2Pt\}^{2+}$, **4** = $\{(NH_3)Pt\}^{2+}$, **4**′ = $\{Pt\}^{2+}$.

imidazole ring of all the histidine residues in the four peptides. The results (Table S4, Figures S1 and S2 in the Supporting Information) show that these histidines are indeed surface-exposed. As His249 binds to Fe^{3+} in holo-hTf and the ruthenated peptide T15 was detected in the tryptic digests of both ruthenated apo- and holo-hTf adducts, His242 is thus most likely the ruthenation site in T15. And in T18, T42, and T45, the binding sites for complexes **1** and **2** are the solvent-accessible histidine His273, His578, and His606, respectively.

The platinated peptide T16 contains an S-donor Met256 and an N-donor His273 (Table S3), of which the former residue has been previously identified as the major binding site for cisplatin by ^{13}C and ^{15}N NMR spectroscopy[37] and multi-dimensional liquid chromatography and ESI tandem mass spectrometry;[36] the latter was identified as the major ruthenation site in this work. Because the platinated peptide T18 (Table S3) contains only the surface-exposed His273 residue (Table S4), the His273 residue is the platination site in T18, while in T16 both Met256 and His273 are possible platination sites. The platinated peptide T43 arising from the tryptic digestion of both platinated apo- and holo-hTf complexes contains N-donors His578 and His585. His585 is one of the ligands for ion binding that was not affected upon the platination, and His578 was also identified as one of the ruthenation sites. Therefore, the platination site in T43 is more likely His578 instead of His585. The platinated peptide T24 contains the O-donor Tyr314 which was previously identified as one of the binding sites for cisplatin in apo-hTf based on the observation of a platinated peptide fragment (aa313)-MYLGYEYVTAIR(aa324) by LC-MS/MS analysis .[36] Apart from Tyr314, this peptide fragment contains two additional tyrosine residues Tyr317 and Tyr319. By analyzing the well-established X-ray crystal structures of apo- and holo-hTf, we found that the hydroxyl oxygen of Tyr314 and Tyr319 has small solvent accessible areas (SAA) in apo-hTf and is deeply buried in holo-hTf, but Tyr317 is surface-exposed with a large SAA in both apo- and holo-hTf (Table S4, Figures S1 and S2). Because the platinated T24 was detected at a similar level in the tryptic digests of both platinated apo-hTf and holo-hTf adducts, the Tyr317 is most likely the platination site in T24.

There are not putative cisplatin binding sites available in the platinated peptide T10. Instead, there is an O-donor Tyr136 surface-exposed in both apo- and holo-hTf (Table S4, Figures S1 and S2). Taking the affinity of Tyr317 to cisplatin in T24 into account, the Tyr136 residue appears to be the platination site in T10.

The platinated peptide T34 was only detected in the tryptic digest of the apo-hTf–cisplatin complex. There are an S-donor Met464 and two O-donor Thr457 and Tyr468 in T34. The Met464 residue was completely buried in apo-hTf, and the hydroxyl oxygen of Tyr468 is surface-exposed in both apo- and holo-hTf but has a smaller SAA in apo-hTf (15.9 Å) than in holo-hTf (29.1 Å). In contrast, the hydroxyl oxygen of Thr457 has a large SAA in apo-hTf (37.8 Å) but is completely buried in holo-hTf (Figure 3 and Figure S3, Table S4). These suggest that the O-donor Thr457 is most probably one of the platination sites in apo-hTf, in line with previous reports.[35,36]

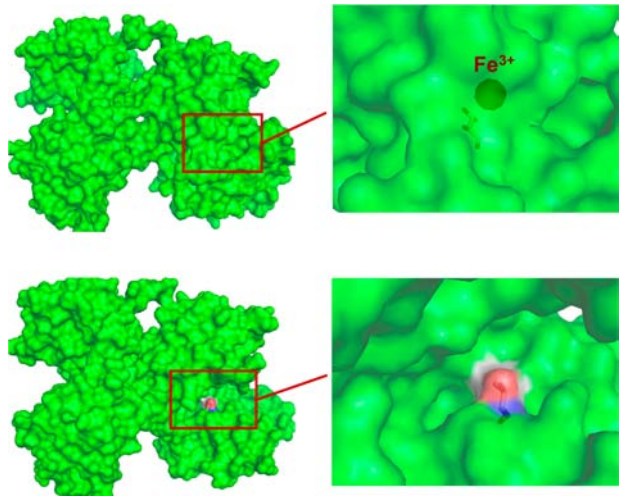

Figure 3. The conformation of the iron-binding site in the C-lobe of holo-hTf (top) and apo-hTf (bottom). The residue Thr457 is shown as sticks color-coded by atom type, indicating that the hydroxyl group of the residue is buried in holo-hTf but solvent accessible (Figure S3) in apo-hTf. On the basis of the X-ray structure of holo-hTf (PDB code: 3QYT) and apo-hTf (PDB code: 2HAV), the models were generated using PyMol.

Molecular Modeling. Although complexes **1** and **2** cannot replace iron(III) bound to hTf, complexes **1** and **2** can bind to His242 and His578, which are close to the iron sites in the N-lobe and the C-lobe of holo-hTf, respectively. Cisplatin can also coordinate to His578 in holo-hTf, and to Thr457, which is located within the iron site of the C-lobe in apo-hTf. To evaluate the effect of the Ru and Pt bindings on the conformation of hTf, we constructed molecular models of

dx.doi.org/10.1021/ic4002626 | Inorg. Chem. 2013, 52, 5328−5338

ruthenated/platinated hTf adducts using the Surflex docking module of Sybyl X 1.0 program. As shown in Figure 4 and

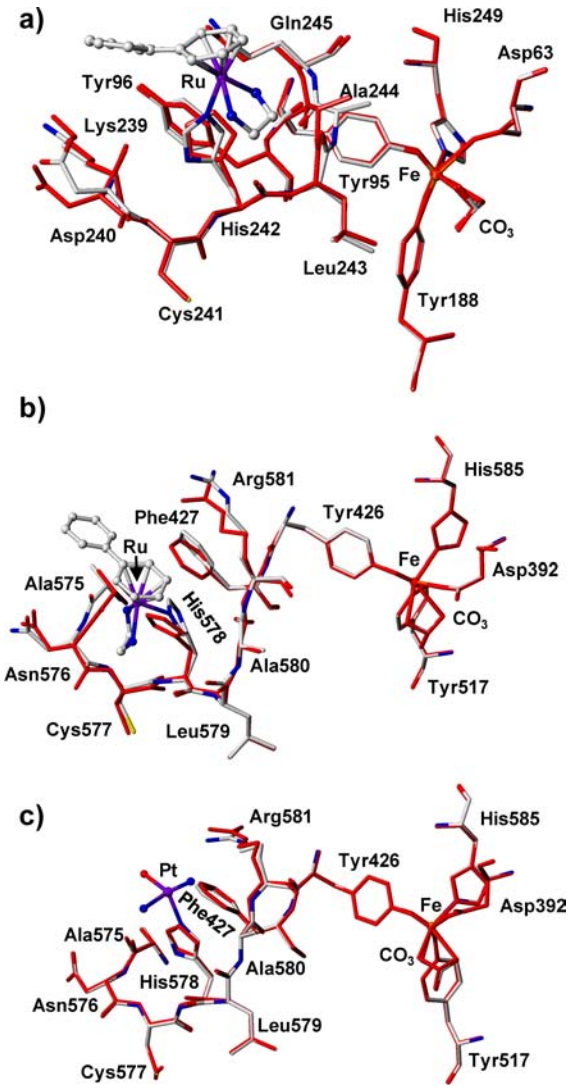

Figure 4. Superposition of the iron-binding site in (a) the N-lobe and (b,c) the C-lobe of native holo-hTf (PDB ID code 3QYT, magenta) and in the energy-minimized model with $\{(\eta^6\text{-bip})Ru(en)\}^{2+}$ (CPK coloring) binding to His242 (a) and His578 (b), and $\{(NH_3)_2Pt(H_2O)\}^{2+}$ (CPK coloring) binding to His578 (c), respectively.

Figure S4, the bindings of ruthenium moiety $\{(\eta^6\text{-arene})Ru(en)\}^{2+}$ (arene = *p*-cym or bip) to His242 and His578 have no pronounced effect on the conformation of the respective iron sites in holo-hTf (PDB code: 3QYT),[7] neither does the binding of platinum moiety $\{(NH_3)_2Pt(H_2O)\}^{2+}$ to His578. However, the coordination of cisplatin to Thr457 of apo-hTf (PDB code: 2HAV)[46] appears to block the iron-binding pocket in the C-lobe (Figure 5), though the Pt coordination does not apparently change the conformation of the iron site and positions of the residues which coordinate to iron(III) in holo-hTf (Figure S5). These suggest that cisplatin may inhibit iron binding to the C-lobe by coordination to Thr457, in agreement with the previous report.[35]

Receptor Binding of Ruthenated and Platinated hTf Complexes. To find out whether the ruthenation and platination of holo-hTf by complexes **1**, **2**, and cisplatin interfere with the interaction between holo-hTf and TfR, we

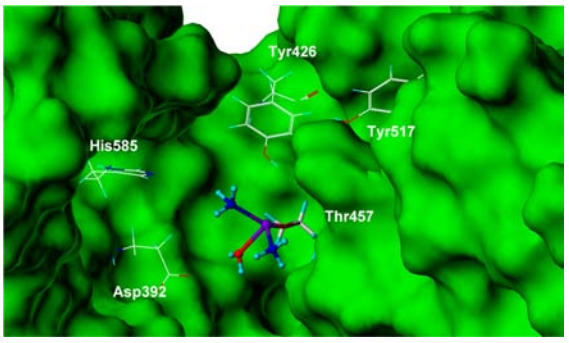

Figure 5. The detailed conformation of cisplatin fragment $\{(NH_3)_2Pt(H_2O)\}^{2+}$ (CPK coloring) binding to Thr457 in the C-lobe of apo-hTf (PDB code: 2HAV). The residues Thr457 as well as the residues Asp392, Tyr426, Tyr517, and His585 which form the iron site are shown in sticks with H atoms in navy blue, O atoms in red, N atoms in blue, and C atoms in gray.

applied the classic receptor assay, the enzyme-linked immunosorbent assay (ELISA), to characterize the interactions of TfR with the ruthenated and platinated holo-hTf complexes, designated as hTf+**1**, hTf+**2**, and hTf+**3** (**3** = cisplatin). The ELISA assays were conducted using the soluble extracellular fragment of human transferrin receptor 1 (hTfR-1) isolated from serum, which retains its capacity to bind differric hTf. The binding curves of native holo-hTf and ruthenated/platinated holo-hTf to hTfR-1 are shown in Figure S6 in the Supporting Information. The EC_{50} values, which correspond to the concentration of a ligand where 50% of its maximal binding to its receptor is observed, are calculated to be 1.67, 1.55, 1.73, and 1.63 μg(hTf) mL^{-1} for native holo-hTf, hTf+**1**, hTf+**2**, and hTf+**3**, respectively. These indicate that neither the ruthenation nor the platination of the holo-hTf protein have pronounced effects on the recognition of holo-hTf by TfR.

To further investigate the influence of the bindings of the ruthenium complexes and cisplatin to diferric transferrin on the interactions between holo-hTf and hTfR, we also used fluorescence confocal microscopy to monitor the internalization of native holo-hTf and ruthenated/platinated holo-hTf to MCF-7 human breast cancer cells and L-02 human normal liver cells. It is known that transferrin is initially internalized via the TfR-mediated endocytosis from clathrin-coated invaginations on the plasma membrane where it eventually detaches to form clathrin-coated vesicles.[47] As shown in Figure 6a, the vesicles containing the tetramethylrhodamine (TMR)-labeled native holo-hTf or ruthenated/platinated holo-hTf adducts were seen to traffic to a region of the perinuclear vesica in MCF-7 cells after 2 h of incubation. Moreover, the internalizations of ruthenated and platinated holo-hTf appear to occur at a similar rate to that of the native holo-hTf, again indicating that the ruthenation and the platination of holo-hTf have little effect on the internalization of hTf mediated by its receptor. As normal cells express less transferrin receptors, hTf is expected to be internalized at a lower level in normal cells than in cancer cells. Indeed, we verified that less TRM-labeled holo-hTf entered L-02 cells via the TfR-mediated endocytosis process and that the ruthenation and the platination of holo-hTf had no significant influence on the internalization of holo-hTf to L-02 cells (Figure 6b).

Cellular Uptake and Cytotoxicity of Ruthenium Arene Complexes and Cisplatin Ligated with hTf. In order to verify the effect of the ligation of the ruthenium complexes and

dx.doi.org/10.1021/ic4002626 | *Inorg. Chem.* 2013, 52, 5328−5338

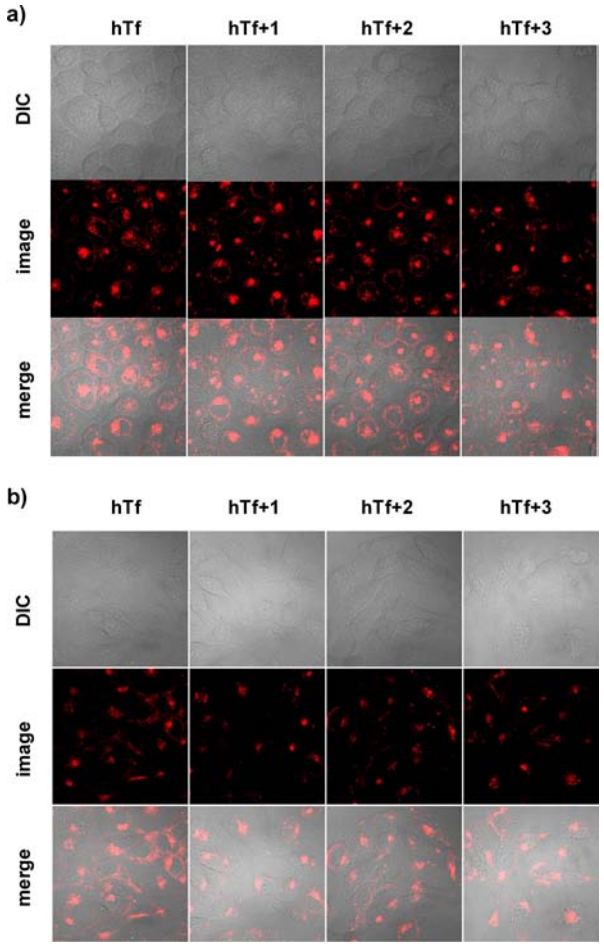

Figure 6. Fluorescent images of (a) MCF-7 cancer cells and (b) L-02 healthy cells exposed to TMR-labeled native, ruthenated and platinated holo-hTf, designated as hTf+**1**, hTf+**2**, and hTf+**3**, respectively, at 310 K for 2 h. The merged images of TMR (red) fluorescent images with differential interference contrast (DIC) images were used to localize TMR-labeled proteins inside cells. Emission at 580 nm and excitation at 555 nm.

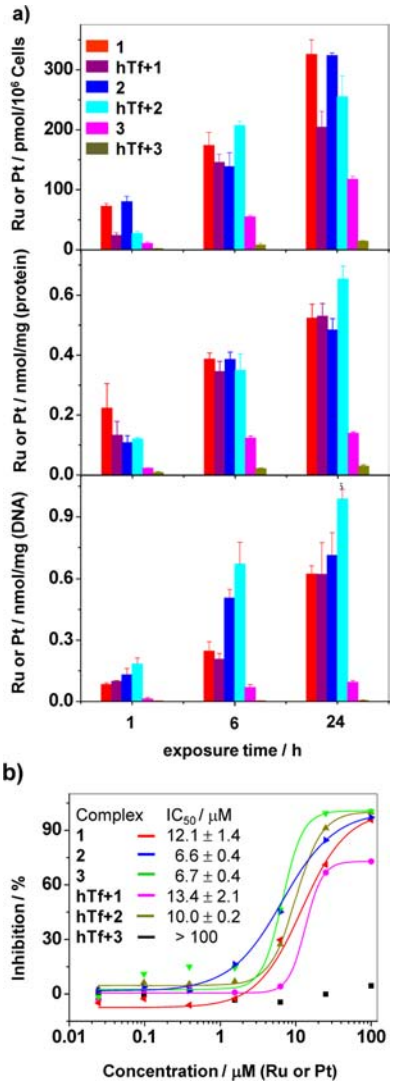

Figure 7. (a) The concentration of cellular (top), protein-bound (middle), and DNA-bound (bottom) Ru or Pt in MCF-7 cancer cells exposed to 20 μM (Ru or Pt) of complexes **1**, **2**, cisplatin (**3**) or their conjugates with holo-hTf (hTf+**1**, hTf+**2**, and hTf+**3**) for various times followed by 24 h of incubation in a drug-free medium. (b) Dose-dependent inhibition curves of complexes **1**, **2**, and cisplatin (**3**) and their conjugates with holo-hTf on growth of MCF-7. The determined IC50 values are shown in the inset. All results are mean of three independent measurements and are expressed as mean ± SD.

cisplatin with hTf on the cellular uptake and bioavailability of these complexes, the cellular uptake and subcellular distribution of the hTf-bound complexes were determined by means of inductively coupling plasma mass spectrometry (ICP-MS) in comparison to those of complexes themselves. As shown in Figure 7a, the intracellular ruthenium concentrations corresponding to the cellular uptake of complexes **1** and **2** ligated with hTf (hTf+**1** and hTf+**2**) are slightly lower than those corresponding to internalization of the complexes themselves, in particular after 24 h of incubation. However, the ruthenated protein adducts formed intracellularly by hTf+**1** and hTf+**2** were at a similar level to those formed by free **1** and **2**. Interestingly, the contents of DNA-bound ruthenium resulting from the reactions of internalized hTf+**2** with DNA are slightly higher than those formed by complex **2** itself, while the ligation with hTf has no effect on the DNA binding of complex **1**. In contrast, the ligation of cisplatin with hTf significantly reduces its cellular uptake, inhibiting the formation of protein and DNA adducts of cisplatin in MCF-7 cells (Figure 7a). The DNA-bound platinum was barely detected in MCF-7 cells exposed to hTf-bound cisplatin (Figure 7a).

As both cisplatin and ruthenium arene complexes are thought to act by attacking DNA, these results described above suggest that ligation with holo-hTf will reserve the cytotoxicity of ruthenium complexes **1** and **2** but reduce that of cisplatin. Indeed, the cytotoxicity assay (Figure 7b) demonstrated that the hTf-bound **1** or **2** showed a similar inhibitory potency on the growth of MCF-7 cancer cells to that of the respective free complex but that the ligation with hTf dramatically reduced the cytotoxicity of cisplatin against MCF-7. The hTf-cisplatin is actually inactive toward MCF-7.

DISCUSSION

Mass Spectrometry for Characterization of Ruthenation/Platination Sites on Transferrin. Hybrid analytical techniques, in particular, electrospray ionization mass spectrometry (ESI-MS) coupled to HPLC, have been widely used to investigate the interactions between metallodrugs and targeted proteins, providing insights into the roles of such

dx.doi.org/10.1021/ic4002626 | Inorg. Chem. 2013, 52, 5328−5338

proteins in the action of metallodrugs.[34] However, for relatively large proteins such as albumin and transferrin, a precise mapping on the metallodrug−protein adducts by LC-ESI-MS can still be a major challenge.[35,36]

To perform an effective identification of metal-binding sites in protein complexes by LC-ESI-MS, the metal−protein coordination bond must exhibit a high thermodynamic stability during both the tryptic digestion at pH ∼8.0 and the subsequent HPLC separation at pH ∼2.3.[36,48] Both cisplatin and ruthenium(II) arene complexes were shown to be able to displace zinc bound to cysteine residues in metallothioneine (MT) at low pH (∼3).[49] The S-donor ligand Met256 residue in holo-hTf was established as the major binding site for cisplatin by ESI tandem mass spectrometry combined with tryptic digestion and multidimensional liquid chromatography.[36] These suggest that Pt^{II} and Ru^{II} bindings to the S-donor ligands are thermodynamically stable at low pH. However, using ESI-MS in conjugation with tryptic digestion and molecular modeling, Dyson and co-workers[35] demonstrated that the threonine-457 residue in apo-hTf instead of Met256 is the major platination site by cisplatin. It was suggested that cisplatin binds weakly to Met256 and that the S−Pt bond is broken during the enzymatic digestion and/or MS analysis of the tryptic peptides.[35] In the present work, we demonstrate that both Ru-coordination with N-donor histidines and Pt-coordination with S-donor, N-donor, and O-donor residues in hTf are strong enough to allow the identification of these metalated peptides by ESI-MS following the reverse phase HPLC separation of the tryptic peptide mixtures, though the neutral loss of coligands in the metal complexes, e.g., NH_3 in cisplatin (Table S3), occurred during the primary mass spectrometry analysis, in line with the previous reports.[36,50,51]

The major challenge for an effective characterization of metalation sites in a relative large protein like hTf is that some metalated peptides may be missed due to the low sequence coverage of identified proteolytic peptides for the targeted protein.[36,48] In general, in order to reduce the potential dissociation and/or replacement of metal−protein bonds, the use of a high concentration of denaturing reagents such as guanidine hydrochloride and disulfide-cleaving reagents such as dithiothreitol (DTT) should be avoided during the proteolytic digestion of protein complexes. As a consequence, the sequence coverage for a large protein might be further reduced and significantly restrict the number of detectable binding sites in a particular protein complex.[36] Recently, by comparing the MS signal intensities of platinated MT incubated with a high concentration of DTT for various times to those of platinated MT without incubation with DTT, we verified that DTT reduced the coordination of Pt to MTs at a certain level, suggesting that DTT as a reducing agent at high concentrations may cause the dissociation of protein-bound metallodrugs.[49] However, upon using selenocystamine dihydrochloride as a catalyst for the cleavage of disulfide bonds of albumin by DTT, the reaction time can be shortened to be 5 min. In this case, the majority of Pt-albumin binding, including a Pt-thiol binding, remained intact during the tryptic digestion.[51] In the present work, using 5 mM of DTT as the reducing agent in the presence of selenocystamine dihydrochloride, 50 tryptic peptides of hTf were identified. These peptides cover approximately 75% of the protein sequence (Table S1), and this sequence coverage is significantly higher than that reported previously,[36] indicating that 75% of ruthenation/platination sites in the metalated hTf could be detected by LC-ESI-MS. In fact, in this work, the potential cisplatin binding sites in hTf identified previously by NMR and MS in conjugation with tryptic digestion in the absence of DTT are all included in the identified platinated peptides. These include Met256,[36,37] Glu265,[36] Tyr314,[36] Glu385,[36] Thr457,[35,36] and Met499[37] (Table S1), though the Glu265, Tyr314, Glu385, and Met499 residues appeared not to be preferential binding sites for cisplatin according to our molecular modeling study (Figures S1 and S2). However, it is worth pointing out that even with high sequence coverage, MS analysis cannot rule out metal coordination to a specific peptide, in particular a low abundant metalated peptide, due to the bias for metal-containing peptides in the mass spectrometer.

The characteristic isotopic distribution of ruthenium and platinum allows quick distinguishing of ruthenated and platinated peptides from complicated peptide mixtures by MS.[36,48,50,51] However, MS data do not allow an unambiguous identification of metalated sites in specific peptides. Tandem mass spectrometry (MS/MS) is a powerful tool to localize the binding sites of metal ions or complex moieties in a particular peptide.[36,51] Alternatively, the chemical modification of side chains of specific binding sites in proteins can also be helpful to the localization of metal-binding sites in the targeted proteins.[50] In this work, we combined the modeling analysis of the well-established X-ray crystal structures of hTf to assist the localization of the ruthenation and platination sites in the metalated peptides. This approach allowed us to localize four binding sites for the ruthenium(II) arene complexes in both apo- and holo-hTf, five and six platination sites by cisplatin in apo- and holo-hTf, respectively. These suggest that the combined application of LC-MS with tryptic digestion of metalated protein adducts and in silico analysis of the crystal structures of targeted proteins is an effective alternation for determining the binding sites of metallodrugs to proteins.

Coordination Chemistry of Ruthenium and Platinum Bindings to hTf. Although it is still argued whether Fe^{3+}-binding at the C-terminal lobe is essential for receptor recognition or merely an event that precedes N-terminal lobe iron binding, the diferric hTf (Fe_2Tf) binds to TfR more strongly than the apo (apo-hTf) and the monoferric forms (Fe_NTf and Fe_CTf with the metal-containing lobe indicated by the subscript N and C) of the protein. At the extracellular pH 7.4, the receptor binding constants of Fe_2Tf−TfR is at least an order of magnitude larger than those of Fe_NTf and Fe_CTf to TfR.[52] Very recently, Jensen et al. reported that the Fe_NPu_CTf complex, where the plutonium(IV) ion binds in the C-lobe and iron(III) binds in the N-lobe, binds to TfR more strongly than the Pu_NFe_CTf and Pu_2Tf complexes.[53] This implies that the C-lobe of hTf can be closed upon the bindings of other metal ions, forming the proper conformation being recognized by TfR.

Due to the similarity between Fe^{3+} and Ru^{3+}, e.g., similar ion radius and coordination geometry and similar hardness as hard Lewis acids, the ruthenium(III) anticancer complex $[Ru^{III}Cl_4(Ind_2)]$HInd (KP1019, Ind = indazole) has been shown to bind preferentially to the iron sites in hTf. However, unlike iron(III) complexes such as Fe(EDTA) and Fe(nitrilotriacetate), KP1019 kept its indazole ligands intact when binding to apo-hTf.[8,39] As a consequence, the binding of KP1019 to apo-hTf did not induce the formation of the proper conformation, which can be recognized by TfR, evidenced by a lower cellular uptake of KP1019 in complexation with apo-hTf than that of the complex itself. The bivalent ruthenium ion is

dx.doi.org/10.1021/ic4002626 | Inorg. Chem. 2013, 52, 5328−5338

categorized as a soft Lewis acid, though Ru^{II} complexes adopt an octahedral geometry similar to Fe^{III} compounds. The softness of the Ru^{II} center in the complexes **1** and **2** further increases due to the bulky π-electron-rich arene ligands which are soft Lewis bases. Therefore, the Ru^{II} arene complexes have a higher affinity to the soft bases cysteine and methionine[42,43,49,50] and the borderline base histidine[45,50] than to the hard base glutamic acid, though the coordination of the ruthenium arene complexes to the O-donor glutamic acid appeared to be kinetically favored.[43] In this work, we found that ruthenium(II) in both complexes **1** and **2** only binds to the N-donor ligands, and the molecular modeling (Figure 4 and Figure S4) demonstrates that the bindings of complexes **1** and **2** to His242 and His587 nearby the N-lobe and C-lobe iron(III) sites, respectively, do not affect the conformation of the respective iron sites. These are supported by the similarity between the EC_{50} values (Figure S6) of holo-hTf-(arene)Ru(en) complexes and holo-hTf binding to TfR, and by the similarity between internalization rates of holo-hTf−(arene)Ru(en) complexes and holo-hTf via TfR-mediated endocytosis into MCF-7 cancer cells and L-02 healthy cells (Figure 6). Moreover, conjugation with Fe_2-hTf exhibits little effect on the cellular uptake and bioavailability of complexes **1** and **2** (Figure 7a). And the amounts of intracellular ruthenated DNA adducts in MCF-7 cells treated by **1** or **2** ligated with Fe_2-hTf even increased slightly, compared to those detected in MCF-7 cells exposed to the same concentration of complex **1** or **2** itself. These indicate that the bindings of complexes **1** and **2** to hTf are irreversible and that the protein-bound (arene)Ru(en) units can be released in endosomes, as happened to the hTf-bound ruthenium(III) complex KP1019 which bound to the iron sites in hTf.[9]

The platinum(II) ion is larger in radius (0.94 Å) than Fe^{3+} (0.65 Å),[54] and Pt^{II} compounds are in a square-planar geometry, differing from the octahedral geometry of iron(III) compounds. In the theory of hard and soft acid/base (HSAB), Pt^{2+} is also a soft Lewis base and preferentially coordinates to soft Lewis bases such as the S-donors cysteine and methionine and the borderline base histidine in proteins.[49,51] These features of platinum ions may account for the lack of binding of cisplatin to the specific iron sites, which contain hard bases aspartic acid and carbonate and borderline bases tyrosine and histidine, in hTf. Among the five platinated peptides arising from the tryptic digest of the holo-hTf-cisplatin adduct, two peptides (T10 and T24, Table S3) do not contain surface-exposed cysteine, methionine, or histidine residue available for platinum binding. Instead, both the peptides contain a surface-exposed tyrosine residue, Tyr136 in T10 and Tyr317 in T24, respectively. These imply that cisplatin can coordinate to a surface-exposed borderline base tyrosine to give a thermodynamically stable adduct when there is no competition arising from soft bases such as cysteine and methionine residues in a specific region of the protein, in line with the previous report.[35,36] Attributed to the same reason, cisplatin was found to bind to the surface-exposed Thr457 residue in the iron-binding cleft of the C-lobe of apo-hTf where the nearby S-donor Met464 is buried. Notably, although the coordination of cisplatin to Thr457 in apo-hTf has no significant impact on the conformation of the iron-binding site in the C-lobe, the bound cisplatin moiety appears to block the cleft (Figure 5), probably preventing iron(III) from binding to the C-lobe site and in turn interfering with the cellular uptake of Fe^{3+}.[35] However, the binding of cisplatin to surface-exposed His578 nearby the iron-binding site of the C-lobe in holo-hTf displayed no effect on the conformation of the lobe (Figure 4c). Consequently, the binding of cisplatin to holo-hTf did not influence the internalization of holo-hTf via TfR-mediated endocytosis (Figure 6).

Further studies showed that the bindings of cisplatin to hTf are irreversible, evidenced by the significant decrease in the cellular uptake of platinum and the amount of platinated DNA adducts formed in MCF-7 cells treated by the holo-hTf−cisplatin conjugate compared to those in MCF-7 cells exposed to intact cisplatin (Figure 7a). This implies that accompanying the circulation of hTf, the hTf-bound cisplatin was pumped out from the cells.

Biological Implications. Our studies demonstrate that unlike gallium(III) and ruthenium(III) complexes, ruthenium(II) arene complexes **1** and **2** bind to the surface-exposed histidine residues instead of the specific iron sites in hTf, and that the Ru^{II} bindings do not interfere with the iron bindings of the protein. Therefore, the Ru(arene)−Fe_2−hTf complexes can be recognized by TfR and internalized via the TfR-mediated endocytosis at a similar rate to that of Fe_2−hTf. The ruthenium(II) arene complexes have been thought to exert an effect by attacking DNA.[55−57] Therefore, they should escape from the endosomal vesicles to the cytosol for their subsequent diffusion into the nuclei. The sequestering of antineoplastic agents into acidic endosomal vesicles is responsible for drug resistance in cancer cells apart from the effect of the membrane associated efflux transporter proteins, as the sequestering reduces the accumulation of the drugs in the cytosolic compartment.[20] Our results show herein that the content of ruthenated DNA adducts was slightly higher in MCF-7 cells treated by holo-hTf-conjugated complex **1** or **2** than that in MCF-7 cells exposed to the same concentration of free **1** or **2**. This means that the hTf-bound (arene)Ru(en) pharmacophores can be released in endosomes at low pH (5−6) and passed to nuclei through a cytosolic compartment. As a consequence, the Ru(arene)−Fe_2−hTf complexes showed a similar inhibitory potency on the growth of MCF-7 cancer cells to those of the corresponding free complexes. These findings provide a rationale to use iron-loaded hTf as a carrier to deliver the organometallic ruthenium(II) drug candidates and to overcome the potential drug resistance resulting from protein bindings in endosomal and cytosolic compartments.

In contrast, the amount of platinated DNA adducts dramatically reduced in MCF-7 cells treated by holo-hTf-conjugated cisplatin, compared to that detected in MCF-7 cells exposed to the same concentration of free cisplatin. These indicate that the protein-bound cisplatin fragment cannot be released even in endosomes at low pH, and that the capturing of cisplatin by highly abundant proteins such as transferrin may account for the resistance of cancer cells to cisplatin.

■ CONCLUSION

By the combined use of tryptic digestion, LC-ESI-MS, ICP-MS, molecular modeling, receptor assay, and MTT screening, we demonstrated that the organometallic ruthenium(II) anticancer complexes **1** and **2** could bind to the surface-exposed histidine residues (His249, His273, His578, and His606) in both apo- and holo-hTf. These bindings did not affect the recognition of holo-hTf by TfR, and the (arene)Ru(en)−Fe_2−hTf complexes were internalized via TfR-mediated endocytosis at a similar rate to that of Fe_2−hTf. Furthermore, the conjugation with holo-hTf had little effect on the cellular uptake and bioavailability of

dx.doi.org/10.1021/ic4002626 | Inorg. Chem. 2013, 52, 5328−5338

complexes **1** and **2**; the holo-hTf-conjugated **1** and **2** exhibited a similar cytotoxicity to the free complexes toward human cancer cell line MCF-7. It is therefore feasible to use iron-loaded hTf as a mediator for targeted delivery of the organometallic ruthenium(II) anticancer complexes and for circumventing the potential drug resistance resulting from protein bindings in endosomal and cytosolic compartments. In contrast, although cisplatin bound only to the surface-exposed residues in holo-hTf and the bindings did not impact the internalization of holo-hTf, the protein-bound cisplatin could not be released intracellularly, leading to a dramatic reduction of cisplatin cytotoxicity.

■ ASSOCIATED CONTENT

Ⓢ Supporting Information

MS peptides mapping data (Tables S1−S3) and molecular modeling and receptor assay results (Table S4, Figures S1−S6). This material is available free of charge via the Internet at http://pubs.acs.org.

■ AUTHOR INFORMATION

Corresponding Author

*E-mail: fuyi.wang@iccas.ac.cn.

Notes

The authors declare no competing financial interest.

■ ACKNOWLEDGMENTS

We thank the NSFC (Grant Nos.: 90713020, 20975103, 21020102039, 21135006, and 21127901), the 973 Program of MOST (2013CB531805) for support, Professor Peter J. Sadler and Dr. Abraha Habtemariam of the University of Warwick for stimulated discussion, and Professors Xiaohong Fang and Dihua Shangguan at the Institute of Chemistry, Chinese Academy of Sciences for assistance with cell culture and ELISA experiments.

■ REFERENCES

(1) Gomme, P. T.; McCann, K. B. *Drug Discovery Today* **2005**, *10*, 267−273.
(2) Sun, H. Z.; Li, H. Y.; Sadler, P. J. *Chem. Rev.* **1999**, *99*, 2817−2842.
(3) Qian, Z. M.; Li, H. Y.; Sun, H. Z.; Ho, K. *Pharmacol. Rev.* **2002**, *54*, 561−587.
(4) Harris, W. R.; Messori, L. *Coord. Chem. Rev.* **2002**, *228*, 237−262.
(5) Jameson, G. B.; Anderson, B. F.; Norris, G. E.; Thomas, D. H.; Baker, E. N. *Acta Crystallogr., Sect. D: Biol. Crystallogr.* **1998**, *54*, 1319−1335.
(6) Sun, X. L.; Baker, H. M.; Shewry, S. C.; Jameson, G. B.; Baker, E. N. *Acta Crystallogr., Sect. D: Biol. Crystallogr.* **1999**, *55*, 403−407.
(7) Yang, N.; Zhang, H. M.; Wang, M. J.; Hao, Q.; Sun, H. Z. *Sci. Rep.* **2012**, *2*, 999.
(8) Kratz, F.; Hartmann, M.; Keppler, B.; Messori, L. *J. Biol. Chem.* **1994**, *269*, 2581−2588.
(9) Pongratz, M.; Schluga, P.; Jakupec, M. A.; Arion, V. B.; Hartinger, C. G.; Allmaier, G.; Keppler, B. K. *J. Anal. At. Spectrom.* **2004**, *19*, 46−51.
(10) Jakupec, M. A.; Galanski, M.; Arion, V. B.; Hartinger, C. G.; Keppler, B. K. *Dalton Trans.* **2008**, 183−194.
(11) Chitambar, C. R.; Wereley, J. P.; Matsuyama, S. *Mol. Cancer Ther.* **2006**, *5*, 2834−2843.
(12) van Leeuwen-Stok, A. E.; Schuurhuis, G. J.; Drager, A. M.; Visser-Platier, A. W.; Teule, G. J.; Huijgens, P. C. *Br. J. Cancer* **1996**, *74*, 619−624.
(13) Bernstein, L. R.; van der Hoeven, J. J. M.; Boer, R. O. *Med. Chem.* **2011**, *11*, 585−590.
(14) Chitambar, C. R. *Curr. Opin. Oncol.* **2004**, *16*, 547−552.
(15) Harris, W. R.; Chen, Y.; Wein, K. *Inorg. Chem.* **1994**, *33*, 4991−4998.
(16) Sun, H. Z.; Li, H. Y.; Weir, R. A.; Sadler, P. J. *Angew. Chem., Int. Ed.* **1998**, *37*, 1577−1579.
(17) Guo, M. L.; Sun, H. Z.; McArdle, H. J.; Gambling, L.; Sadler, P. J. *Biochemistry* **2000**, *39*, 10023−10033.
(18) Chikh, Z.; Ha-Duong, N. T.; Miquel, G.; Chahine, J. M. E. *J. Biol. Inorg. Chem.* **2007**, *12*, 90−100.
(19) Hummer, A. A.; Bartel, C.; Arion, V. B.; Jakupec, M. A.; Meyer-Klaucke, W.; Geraki, T.; Quinn, P. D.; Mijovilovich, A.; Keppler, B. K.; Rompel, A. *J. Med. Chem.* **2012**, *55*, 5601−5613.
(20) Brigger, I.; Dubernet, C.; Couvreur, P. *Adv. Drug Delivery Rev.* **2002**, *54*, 631−651.
(21) Bruijnincx, P. C. A.; Sadler, P. J. *Adv. Inorg. Chem.* **2009**, *61*, 1−62.
(22) Hartinger, C. G.; Dyson, P. J. *Chem. Soc. Rev.* **2009**, *38*, 391−401.
(23) van Rijt, S. H.; Sadler, P. J. *Drug Discovery Today* **2009**, *14*, 1089−1097.
(24) Yan, Y. K.; Melchart, M.; Habtemariam, A.; Sadler, P. J. *Chem. Commun.* **2005**, 4764−4776.
(25) Bregman, H.; Carroll, P. J.; Meggers, E. *J. Am. Chem. Soc.* **2006**, *128*, 877−884.
(26) Alessio, E.; Mestroni, G.; Bergamo, A.; Sava, G. *Curr. Top. Med. Chem.* **2004**, *4*, 1525−1535.
(27) Hartinger, C. G.; Zorbas-Seifried, S.; Jakupec, M. A.; Kynast, B.; Zorbas, H.; Keppler, B. K. *J. Inorg. Biochem.* **2006**, *100*, 891−904.
(28) Berger, M. R.; Garzon, F. T.; Keppler, B. K.; Schmahl, D. *Anticancer Res.* **1989**, *9*, 761−765.
(29) Habtemariam, A.; Melchart, M.; Fernandez, R.; Parsons, S.; Oswald, I. D. H.; Parkin, A.; Fabbiani, F. P. A.; Davidson, J. E.; Dawson, A.; Aird, R. E.; Jodrell, D. I.; Sadler, P. J. *J. Med. Chem.* **2006**, *49*, 6858−6868.
(30) Morris, R. E.; Aird, R. E.; Murdoch, P. D.; Chen, H. M.; Cummings, J.; Hughes, N. D.; Parsons, S.; Parkin, A.; Boyd, G.; Jodrell, D. I.; Sadler, P. J. *J. Med. Chem.* **2001**, *44*, 3616−3621.
(31) Wang, F. Y.; Habtemariam, A.; van der Geer, E. P. L.; Fernandez, R.; Melchart, M.; Deeth, R. J.; Aird, R.; Guichard, S.; Fabbiani, F. P. A.; Lozano-Casal, P.; Oswald, I. D. H.; Jodrell, D. I.; Parsons, S.; Sadler, P. J. *Proc. Natl. Acad. Sci. U. S. A.* **2005**, *102*, 18269−18274.
(32) Ang, W. H.; Daldini, E.; Scolaro, C.; Scopelliti, R.; Juillerat-Jeannerat, L.; Dyson, P. J. *Inorg. Chem.* **2006**, *45*, 9006−9013.
(33) Nowak-Sliwinska, P.; van Beijnum, J. R.; Casini, A.; Nazarov, A. A.; Wagnieres, G.; van den Bergh, H.; Dyson, P. J.; Griffioen, A. W. *J. Med. Chem.* **2011**, *54*, 3895−3902.
(34) Timerbaev, A. R.; Hartinger, C. G.; Aleksenko, S. S.; Keppler, B. K. *Chem. Rev.* **2006**, *106*, 2224−2248.
(35) Khalaila, I.; Allardyce, C. S.; Verma, C. S.; Dyson, P. J. *ChemBioChem* **2005**, *6*, 1788−1795.
(36) Will, J.; Wolters, D. A.; Sheldrick, W. S. *ChemMedChem* **2008**, *3*, 1696−1707.
(37) Cox, M. C.; Barnham, K. J.; Frenkiel, T. A.; Hoeschele, J. D.; Mason, A. B.; He, Q. Y.; Woodworth, R. C.; Sadler, P. J. *J. Biol. Inorg. Chem.* **1999**, *4*, 621−631.
(38) Sulyok, M.; Hann, S.; Hartinger, C. G.; Keppler, B. K.; Stingeder, G.; Koellensperger, G. *J. Anal. At. Spectrom.* **2005**, *20*, 856−863.
(39) Smith, C. A.; Sutherland-Smith, A. J.; Keppler, B. K.; Kratz, F.; Baker, E. N. *J. Biol. Inorg. Chem.* **1996**, *1*, 424−431.
(40) Berger, I.; Hanif, M.; Nazarov, A. A.; Hartinger, C. G.; John, R. O.; Kuznetsov, M. L.; Groessl, M.; Schmitt, F.; Zava, O.; Biba, F.; Arion, V. B.; Galanski, M.; Jakupec, M. A.; Juillerat-Jeanneret, L.; Dyson, P. J.; Keppler, B. K. *Chem.—Eur. J.* **2008**, *14*, 9046−9057.
(41) Satomi, Y.; Shimonishi, Y.; Hase, T.; Takao, T. *Rapid Commun. Mass Spectrom.* **2004**, *18*, 2983−2988.
(42) Wang, F. Y.; Chen, H. M.; Parkinson, J. A.; Murdoch, P. D.; Sadler, P. J. *Inorg. Chem.* **2002**, *41*, 4509−4523.

(43) Wang, F. Y.; Xu, J. J.; Habtemariam, A.; Bella, J.; Sadler, P. J. *J. Am. Chem. Soc.* **2005**, *127*, 17734−17743.
(44) McNae, I. W.; Fishburne, K.; Habtemariam, A.; Hunter, T. M.; Melchart, M.; Wang, F. Y.; Walkinshaw, M. D.; Sadler, P. J. *Chem. Commun.* **2004**, 1786−1787.
(45) Wang, F. Y.; Bella, J.; Parkinson, J. A.; Sadler, P. J. *J. Biol. Inorg. Chem.* **2005**, *10*, 147−155.
(46) Wally, J.; Halbrooks, P. J.; Vonrhein, C.; Rould, M. A.; Everse, S. J.; Mason, A. B.; Buchanan, S. K. *J. Biol. Chem.* **2006**, *281*, 24934−24944.
(47) Moskowitz, H. S.; Yokoyama, C. T.; Ryan, T. A. *Mol. Biol. Cell* **2005**, *16*, 1769−1776.
(48) Will, J.; Sheldrick, W. S.; Wolters, D. *J. Biol. Inorg. Chem.* **2008**, *13*, 421−434.
(49) Zhang, G. X.; Hu, W. B.; Du, Z. F.; Lv, S.; Zheng, W.; Luo, Q.; Li, X. C.; Wu, K.; Han, Y. M.; Wang, F. Y. *Int. J. Mass Spectrom.* **2011**, *307*, 79−84.
(50) Hu, W. B.; Luo, Q.; Ma, X. Y.; Wu, K.; Liu, J. A.; Chen, Y.; Xiong, S. X.; Wang, J. P.; Sadler, P. J.; Wang, F. Y. *Chem.—Eur. J.* **2009**, *15*, 6586−6594.
(51) Hu, W. B.; Luo, Q.; Wu, K.; Li, X. C.; Wang, F. Y.; Chen, Y.; Ma, X. Y.; Wang, J. P.; Liu, J. A.; Xiong, S. X.; Sadler, P. J. *Chem. Commun.* **2011**, *47*, 6006−6008.
(52) Mason, A. B.; Halbrooks, P. J.; James, N. G.; Connolly, S. A.; Larouche, J. R.; Smith, V. C.; MacGillivray, R. T. A.; Chasteen, N. D. *Biochemistry* **2005**, *44*, 8013−8021.
(53) Jensen, M. P.; Gorman-Lewis, D.; Aryal, B.; Paunesku, T.; Vogt, S.; Rickert, P. G.; Seifert, S.; Lai, B.; Woloschak, G. E.; Soderholm, L. *Nat. Chem. Biol.* **2011**, *7*, 560−565.
(54) Shannon, R. D. *Acta Crystallogr., Sect. A.* **1976**, *32*, 751−767.
(55) Bruijnincx, P. C. A.; Sadler, P. J. *Curr. Opin. Chem. Biol.* **2008**, *12*, 197−206.
(56) Novakova, O.; Kasparkova, J.; Bursova, V.; Hofr, C.; Vojtiskova, M.; Chen, H. M.; Sadler, P. J.; Brabec, V. *Chem. Biol.* **2005**, *12*, 121−129.
(57) Chen, H. M.; Parkinson, J. A.; Novakova, O.; Bella, J.; Wang, F. Y.; Dawson, A.; Gould, R.; Parsons, S.; Brabec, V.; Sadler, P. J. *Proc. Natl. Acad. Sci. U. S. A.* **2003**, *100*, 14623−14628.